COMPARISONS OF THE GROUND MOTION PARAMETERS OF THE LUSHAN EARTHQUAKE WITH EMPIRICAL PREDICTIONS

Yuzhu. Bai[(1)]

[(1)] *Associate Researcher, Institute of Geology, China Earthquake Administration, e-mail: yuzhubai2008@126.com*

Abstract

To study the characteristics of strong ground motion due to the Lushan earthquake, this work first shows the spatial variation of strong ground motion amplitude of the Lushan earthquake. The results indicate that the fastest attenuation direction is through the epicenter from northwest to southeast, which is almost normal to the earthquake fault strike. From northeast to southwest, that is, along the fault strike, the attenuation of the ground-motion component is not so strong. Then, the spatial variation of frequency content parameter of the Lushan ground motion indicates that the topography in the region has significant effect on the distribution of frequency content of ground motion, for example, many small size of basins distributing along the faults lead to enriching in long period strong motion. Moreover, the contour of the significant duration (5-75% ($D_{5\text{-}75}$) and 5-95% ($D_{5\text{-}95}$) of the normalized Arias intensity) shows that the topography in the study region has almost no effect on the variation of $D_{5\text{-}75}$ and $D_{5\text{-}95}$. To further investigate the region-dependence of strong ground motion caused by the Lushan earthquake, the present work also compares the strong ground motion parameters of the Lushan earthquake with median predictions from empirical models that have been developed based on the global earthquake data. The strong ground motion parameters of the Lushan earthquake used to compare include amplitude (the peak ground acceleration (PGA)), frequency content (the mean period (T_m), the predominant spectral period (T_p), the average spectral period (T_{avg}), and the smoothed spectral predominant period (T_o)), and significant duration ($D_{5\text{-}75}$ and $D_{5\text{-}95}$) parameters. The ground motion models (GMMs) used to compare include the recent Next Generation Attenuation (NGA)-West2 GMMs for amplitude, the models of L09 (Lee, 2009), RFRB04 (Rathje et al. 2004), Du17 (Du, 2017), Y-S15 (Yaghmaei-Sabegh, 2015), and RAB98 (Rathje *et al.*, 1998) for frequency content parameters, and the models of KS06 (Kempton and Stewart, 2006), BSA09 (Bommer *et al.*, 2009), G11(Ghanat, 2011), AS16 (Afshari and Stewart, 2016), DW17 (Du and Wang, 2017), L09 (Lee, 2009), and YS14 (Yaghmaei-Sabegh *et al.* 2014) for the significant duration. The comparison results show that the Lushan earhquake has the region-dependence for the amplitude and frequency content parameters of strong ground. There is no region-dependence for the parameters of $D_{5\text{-}75}$ and $D_{5\text{-}95}$ of the Lushan earthquake, which agrees with the recent developed GMMs for the duration defined by the random vibration theory (RVT-duration).

Keywords: *Lushan Earthquake; Ground motion models (GMMs); Strong motion recordings.*

1. Introduction

With the enriching of strong motion data in recent 30 years, the ground motion models (GMMs) for amplitude, frequency content and duration of ground motion due to earthquakes has progressed greatly. The representative GMMs for amplitude of ground motions include the recently development of Next Generation Attenuation (NGA)-West2 models (including the models of the ASK14 (Abrahamson et al., 2014), BSSA14 (Boore et al., 2014), CB14 (Campbell and Bozorgnia, 2014), CY14 (Chiou and Youngs, 2014) and I14 (Idriss, 2014)). The GMMs for frequency content parameters of ground motions are the models of L09 (Lee, 2009), RFRB04 (Rathje et al. 2004), Du17 (Du, 2017), Y-S15 (Yaghmaei-Sabegh, 2015), and RAB98 (Rathje et al., 1998). The GMMs for significant duration of ground motions are the models of KS06 (Kempton and Stewart, 2006), BSA09 (Bommer et al., 2009), G11(Ghanat, 2011), AS16 (Afshari and Stewart, 2016), DW17 (Du and Wang, 2017), L09 (Lee, 2009), and YS14 (Yaghmaei-Sabegh et al. 2014).

The M_w 6.7 Lushan earthquake happened on 20 April 2013 in western Sichuan in China. It was another destructive earthquake that struck the Sichuan Province almost exactly five years after the 2008 Wenchuan earthquake. Its epicenter is at 30.3° N and 103.0° E (Wang *et al.*, 2013) , which is located along the southern segment of the Longmenshan thrust belt and 85 km away from the initial nucleation point/epicenter of the Wenchuan earthquake (Xu *et al.*, 2013), as shown in Figure 1. On the Modified Mercalli (MM) intensity scale, the maximum observed intensity of the Lushan event is MM IX.

The strong motion data from the Lushan earthquake are not included in the development of the previously mentioned GMMs. Moreover, the strong motion data from China included in the global strong motion dataset is not so much. Therefore, the comparison of the amplitude, frequency content, and significant duration of the Lushan earthquake with those predictions by the GMMs is needed to be investigated. The present work firstly show the spatial variation of strong motion parameters of the Lushan event including the amplitude, frequency content, and significant duration parameters. Secondly, the strong motion parameters of the Lushan earthquake are compared with those predicted by the GMMs.

2. Data and Method

The ground motion caused by the Lushan event could be felt in Sichuan, Gansu, Chongqing, Guizhou, Shanxi, and Yunnan provinces in China. In the modified Mercalli intensity scale, the maximum observed intensity of the Lushan event is IX. There were about 200 people killed or missing in this event (Xie et al., 2014). Meanwhile, there were about 15,500 earthquake induced landslide points distributed in the area with the epicenter distance less than 100 km. During the major shock of the Lushan event, a total of 123 strong-motion seismometers were triggered. Most of these recorded data are usable for periods of up to 10 s. Excluded data with late triggers (*S*-wave triggers), spikes, strong noise, or missing components, there are 72 free-field 3-component accelerograms with the site-to-rupture distances (R_{rup}) less than 300 km finally selected and processed (Fig. 1). For all records of the Lushan event, we used the same processing procedure, which included correction for baseline trends and band-pass filtering. We have used non-causal, band-pass Butterworth filters with an order of 4. The selected frequency range is 0.1 to 25 Hz. The lower frequency limit produced well-shaped displacement time series for many records by inspecting. The upper frequency limit was chosen by the spectra characteristics of digitization errors from strong motion accelerograms (Yu *et al.*, 2005). The seismogenic model parameters of the Lushan earthquake are listed in Table 1.

Table 1 – The Rupture Dimensions of the Lushan Earthquake

Seismogenic Model Parameters	**Fault length (km)**	**Fault width (km)**	**Fault strike (degree)**	**Fault dip (degree)**	**Slip angle (degree)**	**Focus depth (km)**	**Fault depth (km)**

Values	66	30	205	38	96	16	9

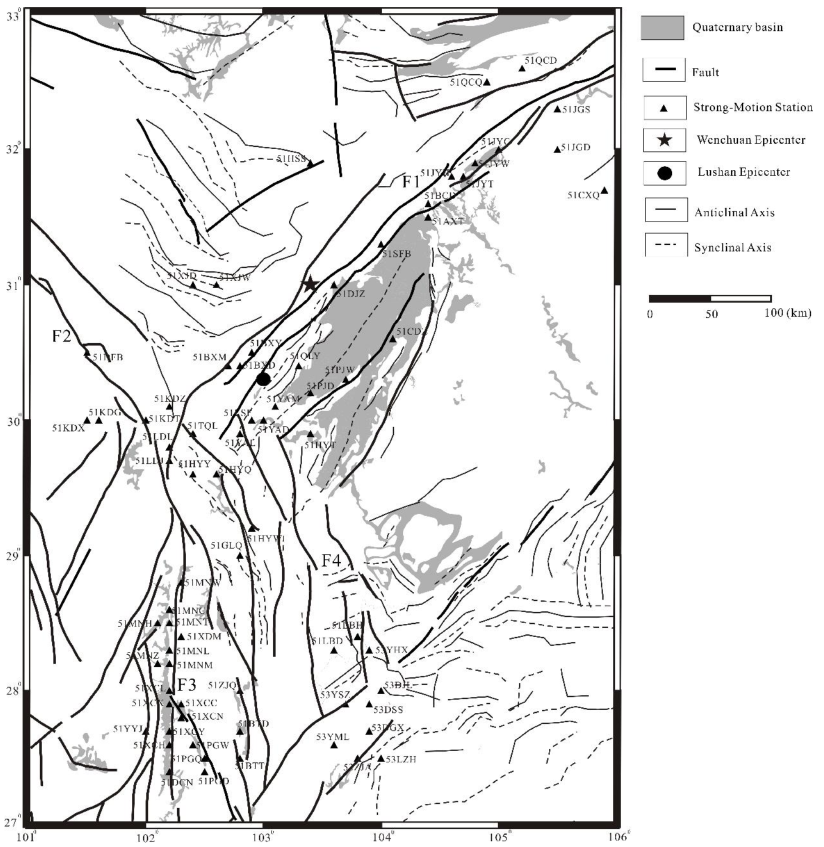

Fig. 1-The station distribution and seismotectonics in the study area. F1 indicates the Longmenshan fault belt; F2 indicates the Xianshuihe fault belt; F3 indicates the Anninghe fault belt; F4 indicates the Yingjing-Mabian fault belt (Bai, 2019).

3. The Spatial Variation of Strong Motion Parameters of the Lushan Earthquake

3.1 The spatial variations of amplitude of strong motions from the Lushan earthquake

Based on the 39 stations with R_{rup} less than 200 km, the distributions of PGA and peak ground velocity (PGV) in space are shown in Figure 2. The contour maps of horizontal (EW and NS) and vertical (UD) PGA and PGV indicate that the maximums of PGA and PGV components are not located at the epicenter. The maximum of UD component of PGV (Fig. 2f) is located to the southwest of the epicenter, whereas the other maximums are located to the northwest of the epicenter. For both PGA and PGV, the fastest attenuation direction is through the epicenter from northwest to southeast, which is almost normal to the earthquake fault strike. From northeast to southwest, i.e. along the fault strike, the attenuation of ground motion component is not so strong. The above facts are speculated to be related to the character of main motion of the Lushan earthquake fault, which is the extrusion movement of the thrust fault.

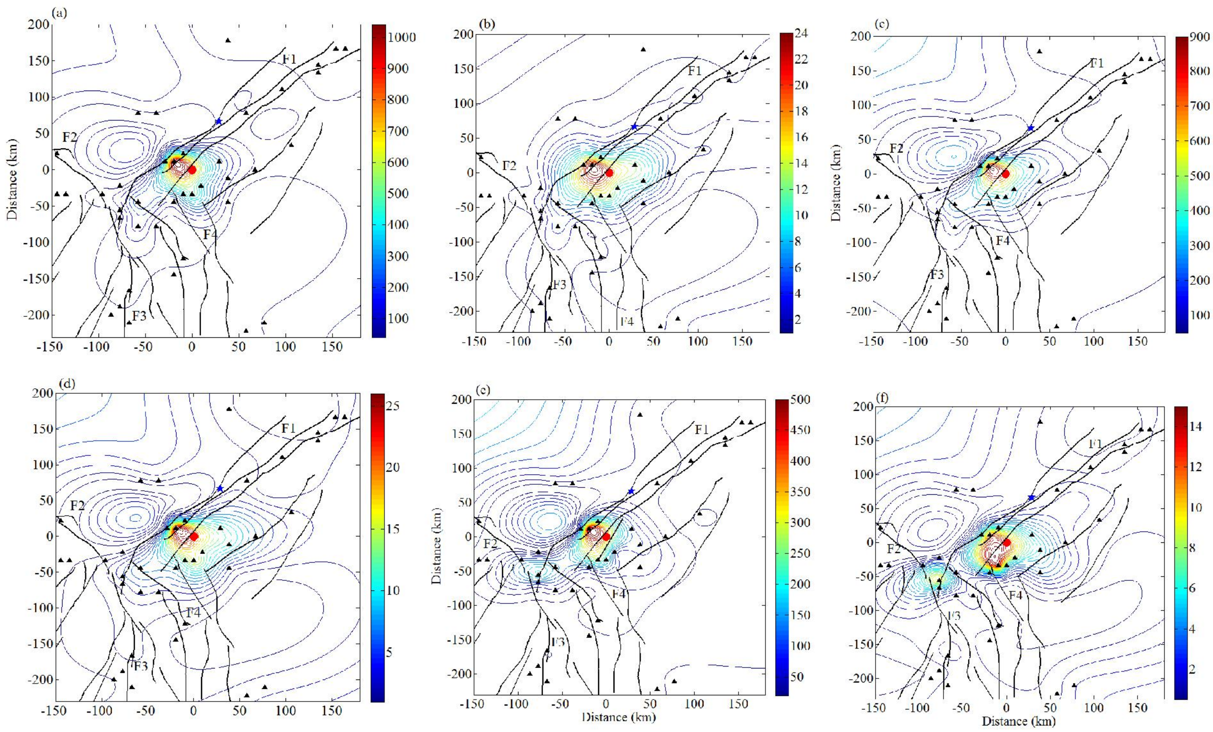

Fig.2 - The contour of PGA (a, c, and e) and PGV (b, d, and f) of the Lushan earthquake with rupture distance less than 200 km. ▲-The strong-motion station; ●- The Lushan earthquake epicenter; ★- The Wenchuan earthquake epicenter; a, c, e, and b,d,f are PGA and PGV component in EW, NS, and UD respectively (Bai, 2017).

3.2 The spatial variations of frequency content parameters of strong motions from the Lushan earthquake

In the present work, the frequency content parameters of strong motions include the predominant spectral period (T_p), the smoothed spectral predominant period (T_o), the average spectral period (T_{avg}), and the mean period (T_m) (Rathje et al. 2004). Figure 3 shows the contour maps of T_p, T_m, T_o and T_{avg} in the study area. In general, the shapes of these contour maps approximate, which means that all parameters can characterize the frequency content of the Lushan earthquake to some extent. In Figure 3, T_p, T_m, T_o and T_{avg} show that the long-period (>1 s) ground motions of the Lushan event are almost located at the same regions that are marked by a white ellipse in subfigure of T_p. Overall, the long-period region was observed in the southwest of the study area with R_{rup} > 200 km. In the long-period region, the periods of ground motions increased abruptly. The far-field long-period ground motions are mainly caused by the path and site effects (Du and Wang, 2017), so the geology structures in the study area may be referred to Figure 1. Figure 1 shows that there are many Quaternary basins distributed along strike directions of many large faults in the long-period region. Therefore, the long-period region of the Lushan earthquake was the result of basin effects caused by these Quaternary basins. According to Bai (2017), the Lushan earthquake has the hanging wall effect for the short-period ground motions. When closing to the epicenter, therefore, the ground motions in the hanging wall of the Lushan fault have the relatively shorter period than those in the footwall, as shown in subfigure of T_m and T_o (Fig. 3). Except the long-period region, the periods of the Lushan event do not vary dramatically (Fig. 3), which possibly results from the Lushan earthquake enriching in short-period (<0.8 s).

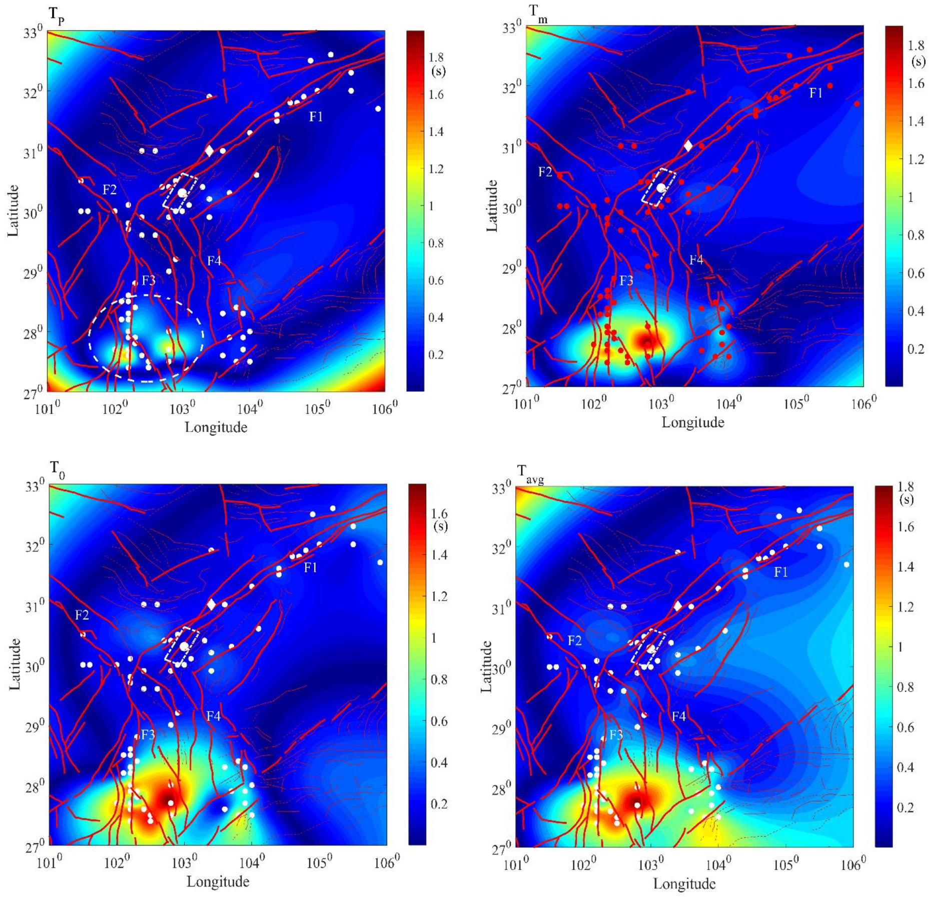

Fig. 3 - The contours of the predominant spectral period (T_p), mean period (T_m), smoothed spectral predominant period (T_0) and averaged spectral period (T_{avg}) for the horizontal component of the Lushan earthquake with rupture distance less than 300km. The big white dot indicates the Lushan epicenter; the white diamond indicates the Wenchuan epicenter; the white rectangle indicates the Lushan fault projection; the little white and red dots indicate the strong-motion stations; the red thick lines indicate the faults; the red solid lines indicate the anticlinal axes; and the red fine dot lines indicate the synclinal axes (Bai, 2018).

3.3 The spatial variations of significant duration of strong motions from the Lushan earthquake

In this study, the significant duration of strong motions includes 5-75% ($D_{5\text{-}75}$) and 5-95% ($D_{5\text{-}95}$) of the normalized Arias intensity. Figure 4 is the contour maps of $D_{5\text{-}75}$ and $D_{5\text{-}95}$ in the study area. The approximation of these maps indicates that $D_{5\text{-}75}$ and $D_{5\text{-}95}$ can character the duration of the Lushan event. Both $D_{5\text{-}75}$ and $D_{5\text{-}95}$ show that the duration near the epicenter of the Lushan event is almost equal to the source duration (Wang *et al.*, 2013). Compared to $D_{5\text{-}75}$, the spatial variation of $D_{5\text{-}95}$ is not dramatically. In the far field, the $D_{5\text{-}95}$ is more affected by geological structure than $D_{5\text{-}75}$, such as in the north-east and south-west of the study area. Moreover, there are more regions for lower $D_{5\text{-}75}$ in the directions parallel to the extrusion and rupture movements of the Lushan earthquake fault (Zhao et al., 2014) than those for $D_{5\text{-}95}$.

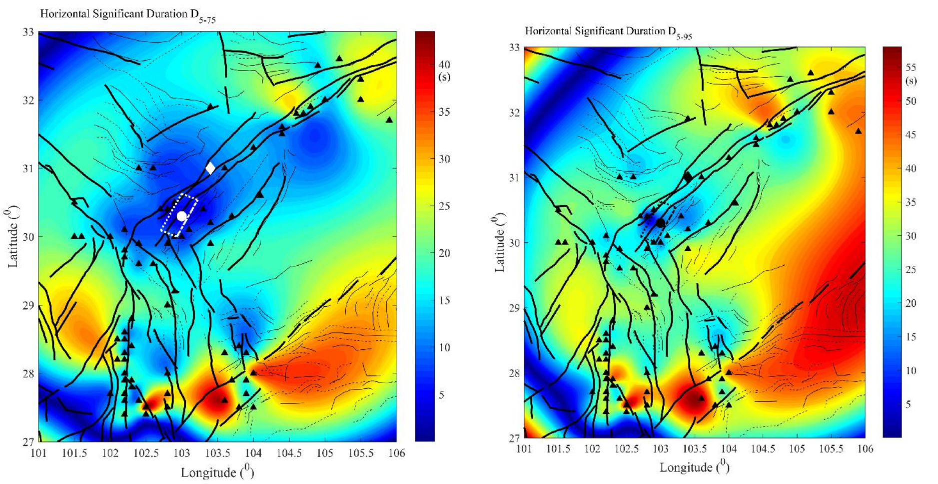

Fig. 4 - The contours of the significant duration ($D_{5\text{-}75}$ and $D_{5\text{-}95}$) for the horizontal component of the Lushan earthquake with rupture distance less than 300km. The big dot indicates the Lushan epicenter; the diamond indicates the Wenchuan epicenter; the rectangle indicates the Lushan fault projection; the triangle dots indicate the strong-motion stations; the black thick lines indicate the faults; the black solid lines indicate the anticlinal axes; and the black fine dot lines indicate the synclinal axes.

4. Comparison of the Recorded Strong Motion Parameters of the Lushan Earthquake with Median Predictions

4.1 Comparison of recorded strong motion amplitude of the Lushan event with NGA West2 GMPEs for R_{rup}

The observed ground motions of PGA are compared with median predictions from the five NGA West2 models as a function of R_{rup} with V_{s30}=700 m/s (Fig. 5), which is around the median value of the V_{s30} from the 39 stations. In order to be consistent with the NGA models, the GMRotI50 of the PGA for the two orthogonally horizontal components of the observed recordings are calculated by the method of Boore's (2006). Additional attention should be paid to that some coefficients of the regionally anelastic attenuation terms/coefficients in the models of ASK14, BSSA14, CB14, and CY14 need to be carefully elected according to the China case. Furthermore, the median predictions plus/minus one standard deviation are indicated as black dash lines in Figure 5. Except for the I14 model, most observed PGA are within one standard deviation of the median prediction. Including the I14 model, almost all the observed values are located in the region between two boundary curves when $R_{rup}\leq$ 40 km. When $R_{rup}>$40 km, more observed values are outside the two boundary curves, although not many. In general, the ASK14 and CY14 model are relatively better at describing the attenuation of the Lushan ground motion among the five GMPEs.

4.2 Comparison of recorded frequecy content of strong motions of the Lushan event with GMMs Predictions for R_{rup}

The recorded T_p, T_m, T_o and T_{avg} are compared with median predictions from the models of L09, Y-S15, DU17, RAB98 and RFRB04 as a function of R_{rup} with V_{S30} = 700 m/s (Fig. 6), which is around the median value of the V_{S30} from 72 stations. Due to the limited data available, it is currently not feasible to investigate the forward-directivity effects. Therefore, such directivity effect is not considered for computing median predictions through these models. Figure 6 indicates that the recorded T_p is the most scattered among the four parameters and the recorded T_{avg} the most concentrated. The distributions of the recorded T_o and T_{avg} show similarities, which results from the same definition of them. For R_{rup} > 200 km, the DU17 model is more consistent with the recorded T_m of the Lushan event. When $R_{rup}\leq$ 200 km, most of the recorded T_p, T_m, T_o and T_{avg} are below all median prediction curves , which is the possible result of the Lushan event enriching in short-period components (Xie et al., 2014). In general, the RFRB04 and L09 models for T_o exhibit more predictive efficiency at describing the frequency content of the Lushan event.

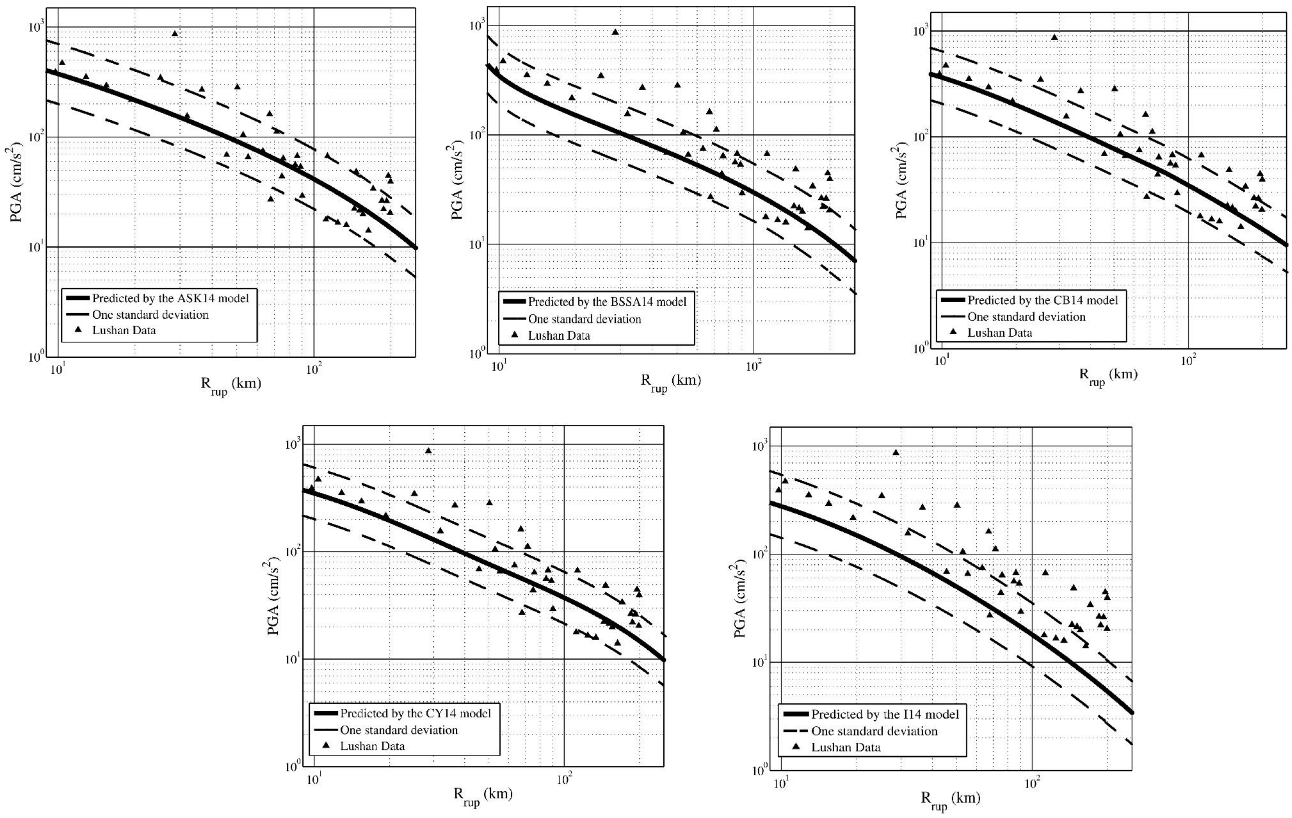

Fig.5 - Comparison of median predictions of PGA from NGA West2 with the corresponding values at the stations of the Lushan event for V_{s30} = 700 m/s. The solid black line is the median prediction by GMPE; the dash black lines in each plot are plus/minus one standard deviation with respect to the GMPE; the black triangle is the station records (Bai, 2017).

4.2 Comparison of the Recorded Significant Duration of the Lushan Earthquake with Predictions from GMMs

In Figure 7, the recorded significant duration from the Lushan event is compared with empirical model predictions as a function of R_{rup} with V_{s30} = 700 m/s, which is around the median value of the V_{s30} from 72 stations. For the Lushan earthquake, the models of DW17, KS06 and AS16 are the best models to characterize $D_{5\text{-}75}$ and $D_{5\text{-}95}$. For $D_{5\text{-}75}$ and $D_{5\text{-}95}$, the DW17 model fits the recorded data of the Lushan event best for R_{rup} < 150 km among the seven GMMs. For $R_{rup} \geq$ 150 km, the L09, KS06, and AS16 models are better at matching the recorded $D_{5\text{-}75}$. For R_{rup} < 150 km, none of the GMMs predict the recorded $D_{5\text{-}95}$ of the Lushan event. The L09 and AS16 models are better to fit the recorded $D_{5\text{-}95}$ for $R_{rup} \geq$ 150 km. For R_{rup} < 150 km, the enrichment of high-frequency components of ground motion (Xie *et al.*, 2014) probably lead to the values of the Lushan significant durations being larger than most of the median predictions. For $R_{rup} \geq$ 150 km, the deficiency of low-frequency components of ground motion probably causes the values of the Lushan $D_{5\text{-}95}$ and $D_{5\text{-}75}$ to be less than the median predictions by the DW17, KS06, and G11models. In Figure 7, most values of $D_{5\text{-}75}$ are larger than the median predictions by the YS14 model, whereas those of $D_{5\text{-}95}$ are smaller. This is probably related to the dataset on which the YS14 model is based. There are only 286 records from 141 earthquakes that are selected to develop the YS14 model (Yaghmaei-Sabegh *et al.*, 2014). Meanwhile, many earthquakes in the dataset have only one record and limited information about source geometry. Therefore, the YS14 model probably has relatively large error. In Figure 7, the recorded duration at the station 51BXD is significantly smaller than the median predictions. It is located on a steep granite hillside (Wen *et al.*, 2013), so the value of V_{s30} at 51BXD is probably much larger than that computed and assigned by the topographic slope data. As a result, the recorded significant duration at 51BXD is significantly smaller than the median predictions based on the small V_{s30}.

However, as the recorded significant duration at the station 51BXD is much smaller than median predictions, as shown in Figure 2, the forward-directivity effects due to the reverse rupture are investigated for this station. First, the length ratio (the fraction of the fault that ruptures towards the site; Somerville *et al.*, 1997; Rathje *et al.*, 2004) for the Lushan fault indicates that forward-directivity effects are unlikely at 51BXD. Second, the method of quantitative classification near-fault ground motions of the 51BXD record (Baker, 2007) is used and no velocity pulse caused by the forward-directivity effects is found. Therefore, the small duration at 51BXD does not result from the forward-directivity effects.

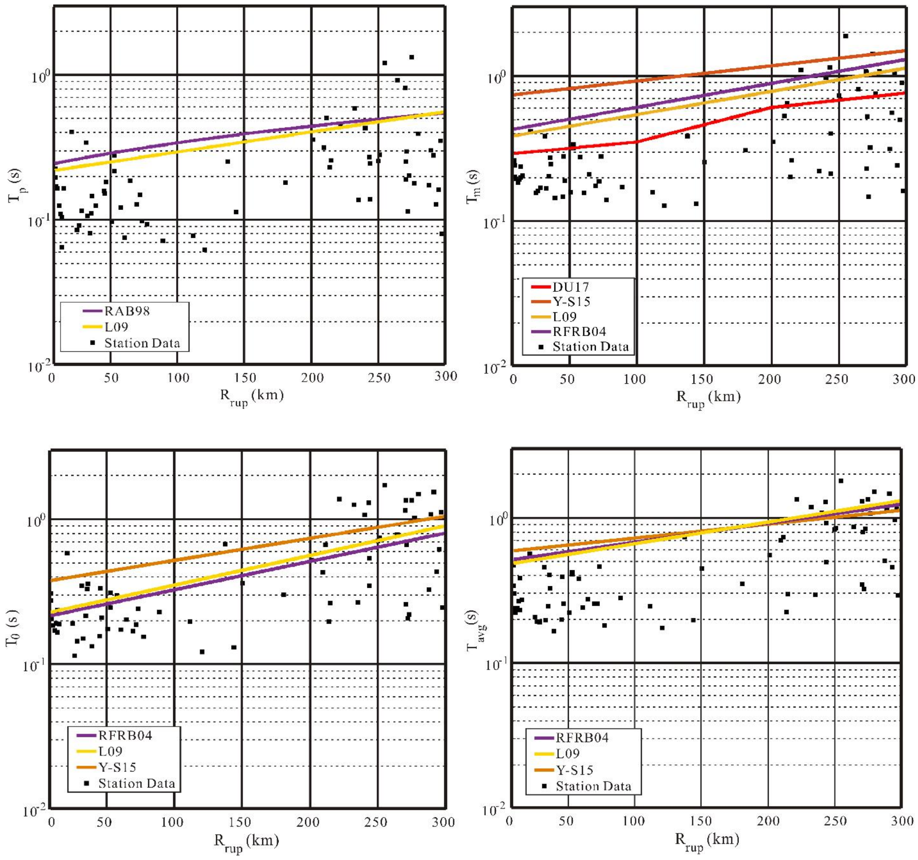

Fig.6 - Comparison of the median prediction of four frequency parameters by the models of RAB98, RFRB04, Y-S15, L09, and Du17 with the recorded values of the Lushan event for V_{S30} = 700 m/s (Bai, 2018).

No GMMs accounting for frequency-dependence have been developed based on global recordings, so the model of NT94 (Novikova and Trifunac (1994)) is selected to compare with the Lushan earthquake recorded $D_{5\text{-}95}$ in 12 separate frequency bands. As illustrated in Figure 8, most of the recorded $D_{5\text{-}95}$ are smaller than predictions for f (frequency) < 1.7 Hz, whereas those for f > 2.5 Hz are larger. Meanwhile, the recorded $D_{5\text{-}95}$ fits relatively well the NT94 model curves in the frequency bands between 1.7 and 2.5 Hz, as shown in Figure 8. In high-frequency bands, such as f > 2.5 Hz, the enrichment of ground motion components lead to the Lushan recorded $D_{5\text{-}95}$ being larger than the predictions. In low-frequency bands, such as f < 1.7 Hz, the deficiency of the ground motion components causes most of the Lushan recorded D_{5-95} to be smaller than the predictions. Moreover, the amount of the Lushan ground motions in bands between 1.7 and 2.5 Hz is probably about average, so the recorded D_{5-95} in these bands matches the NT94 curves well.

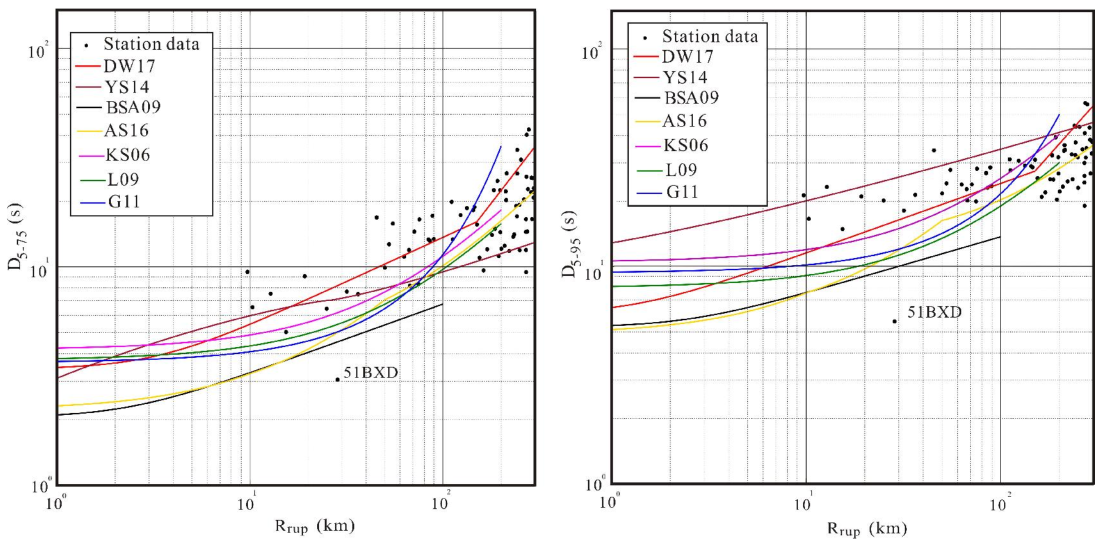

Fig.7 - Comparison of empirical model predictions with the recorded D_{5-75} and D_{5-95} of the Lushan earthquake in horizontal direction for V_{s30}=700m/s (Bai, 2019).

5. Discussion and Conclusion

The present work firstly investigates the spatial variation of the parameters (including the amplitude, frequency content and significant duration parameters) of ground motions from the Lushan earthquake. Then the variation of the ground motion parameters of the Lushan earthquake is compared with the predictions from the representative GMMs. In the work, the forward-directivity effects are stronger for strike-slip events than for dip-slip events (Somerville *et al*., 1997). Strong motion recordings in the near-field of the Lushan earthquake are limited and so the near-fault forward-directivity effects are not included in this comparison study. Through the present work, the main conclusion are following: (1) For both PGA and PGV, the fastest attenuation direction is through the epicenter from northwest to southeast, which is almost normal to the Lushan earthquake fault strike; (2) The geology structures in the Lushan area is the main reason to cause the existing of the long-period region; (3) The significant duration of the Lushan event is relatively less affected by the geology structures in the study area than frequency content parameters; (4) The comparison of the amplitudes of the Lushan event with the empirical prediction indicates that the regional effect will be significantly for R_{rup} > 40 km; (5) The comparison of the frequency content parameters of the Lushan event with the empirical diction shows that the parameter of T_o can be predicted well by the GMMs; (6) The different prediction efficiency on the Lushan earthquake significant duration from the GMMs in different R_{rup} is related to the characters of the ground motion frequency.

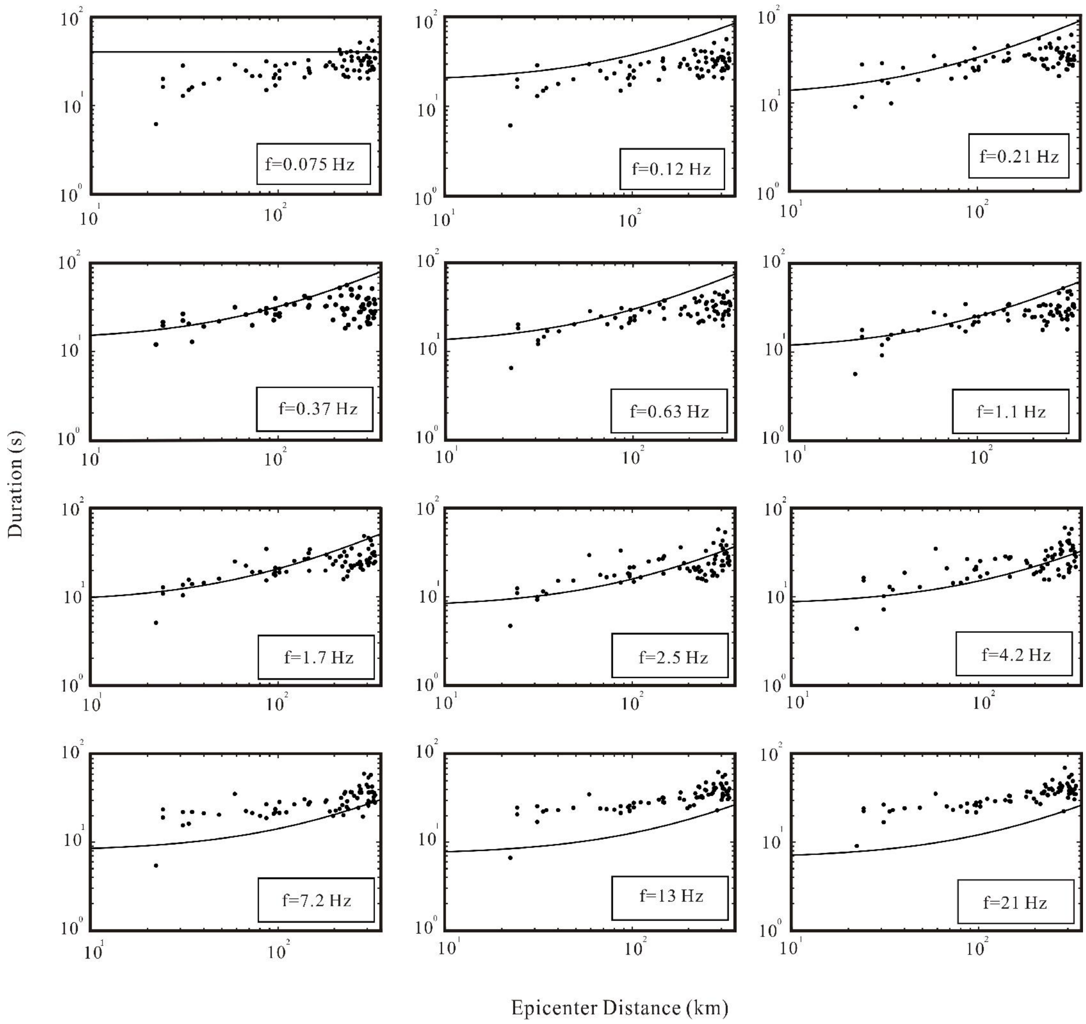

Fig.8 - Comparisons of the recorded $D_{5\text{-}95}$ of the Lushan earthquake in horizontal direction with the NT94 model predictions for 12 frequency bands. The black lines indicate the median predictions by the NT94 model; the black dots indicate the Lushan recording data (Bai, 2019).

6. Acknowledgements

This research was supported by the Basic Research Project of Institute of Geology, China Earthquake Administration (IGCEA1909) and National Key Research and Development Program of China (2018YFC1504703). I appreciate the China Strong Motion Network Sub-Center at Institute of Engineering Mechanics, China Earthquake Administration for providing us with acceleration data of the Lushan.

7. Copyrights

8. References

[1] Abrahamson NA, Silva WJ, Kamai R (2014): Summary of the ASK14 ground motion relation for active crustal regions. *Earthquake Spectra*, **30** (3), 1025-1055.

[2] Boore DM, Stewart JP, Seyhan E, Atkinson GM (2014): NGA-West2 equations for predicting PGA, PGV, and 5% damped PSA for shallow crustal earthquake. *Earthquake spectra*, **30** (3), 1057-1085.

[3] Campbell KW, Bozorgnia Y (2014): Average horizontal components of PGA, PGV, and 5% damped linear acceleration response spectra. *Earthquake Spectra*, **30** (3), 1087-1115.

[4] Chiou BSJ, Youngs RR (2014): Update of the Chiou and Youngs NGA model for the average horizontal component of peak ground motion and response spectra. *Earthquake Spectra*, **30** (3), 1117-1153.

[5] Idriss IM (2014): An NGA-West2 empirical model for estimating the horizontal spectral values generated by shallow crustal earthquakes. *Earthquake Spectra*, **30** (3), 1155-1177.

[6] Lee J (2009): Engineering characterization of earthquake ground motions. *Ph.D. Thesis*, The University of Michigan.

[7] Rathje EM, Faraj F, Russell S, Bray JD (2004): Empirical relationships for frequency content parameters of earthquake ground motion. *Earthquake Spectra*, **20** (1), 119-144.

[8] Du W (2017): An empirical model for the mean period (T_m) of ground motions using the NGA-West2 database. *Bulletin of Earthquake Engineering*, **15** (7), 2673-2693.

[9] Yaghmaei-Sabegh S (2015): New models for frequency contend prediction of earthquake records based on Iranian ground motion data. *Journal of Seismology*, **19** (4), 831-848.

[10] Rathje EM, Abrahamson NA, Bray JD (1998): Simplified frequency content estimates of earthquake ground motions. *Journal of Geotechnical and Geoenvironmental Engineering*, **124** (2), 150-159.

[11] Kempton JJ, Stewart JP (2006): Prediction equations for significant duration of earthquake ground motions considering site and near source effects. *Earthquake. Spectra*, **22** (4), 985-1013.

[12] Bommer JJ, Stafford PJ, Alacrón JE (2009): Empirical equations for the prediction of the significant, bracketed, and uniform duration earthquake ground motion. *Bulletin of the Seismological Society of America*, **99** (6), 3217-3233.

[13] Ghanat S (2011): Duration characteristics of the mean horizontal component of shallow crustal earthquake records in active tectonic regions. *Ph.D. Thesis*, The Arizona State University, Arizona.

[14] Afshari K, Stewart JP (2016): Physically parameterized prediction equations for significant duration in active crustal regions. *Earthquake Spectra*, **32** (4), 2057-2081.

[15] Du WQ, Wang G (2017): Prediction equations for ground-motion significant durations using the NGA-West2 database. *Bulletin of the Seismological Society of America*, **107** (1), 319-333.

[16] Yaghmaei-Sabegh S, Shoghian Z, Sheikh MN (2014): A new model for the prediction of earthquake ground-motion duration in Iran. *Natural Hazards*, **70** (1), 69-92.

[17] Novikova EI, and Trifunac MD (1994): Duration of strong ground motion in terms of earthquake magnitude, epicentral distance, site conditions and site geometry. *Earthquake Engineering & Structural Dynamics*, **23,** (9), 1023-1043.

[18] Wang WM, Hao JL, Yao ZX (2013): Preliminary result for rupture process of Apr. 20, 2013, Lushan earthquake, Sichuan, China. *Chinese Journal of Geophysics*, **56** (4), 1414-1417 (in Chinese).

[19] Xu XW, Wen XZ, Han ZJ, Chen GH, Li CY, Zheng WJ, Zhang SM, Ren ZQ, Xu C, Tan XB, Wei ZY, Wang MM, Ren JJ, He ZT, Liang MT (2013): Lushan Ms7.0 earthquake: A blind reserve-fault event. *Chinese Science Bulletin*, **58** (20), 1887-1893.

[20] Bai YZ (2017): Comparison of strong ground motion recordings of the Lushan, China, earthquake 20 April 2013 with the Next Generation Attenuation (NGA) - West2 ground-motion models. *Bulletin of the Seismological Society of America*, **107** (4), 1724-1736.

[21] Boore DM, Lamprey JW, Abrahamson NA (2006): Orientation-independent measures of ground motion. *Bulletin of the Seismological Society of America*, **94** (4A), 1502-1511.

[22] Xie JJ, Li XJ, Wen ZP, Wu CQ (2014): Near-source vertical and horizontal strong motion from the 20 April 2013 Mw6.8 Lushan earthquake in China. *Seismological Research Letter*, **85** (1), 23-33.

[23] Yu HY, Xie LL, Gong MS (2005): Elimination method and analysis software of digitization errors from the processing of digitizing strong motion accelerograms. *Earthquake Engineering and Engineering Vibration*, **25** (5), 1-5.

[24] Bai YZ (2018): Comparison of the recorded frequency content parameters of the 2013 Lushan earthquake with empirical model predictions. *Bulletin of the Seismological Society of America*, **108** (6), 3358-3367.

[25] Zhao X, Huang ZB, Fang LH, Li Q, Zhao B, Miao CL (2014): Kinematic characteristics of the source process of the Lushan, Sichuan M_s 7.0 earthquake on 20 April 2013. *Chinese Journal of Geophysics*, **57** (2), 419-429.

[26] Somerville PG, Smith NF, Graves RW, Abrahamson NA (1997): Modification of empirical strong ground motion attenuation relations to include the amplitude and duration effects of rupture directivity. *Seismological Research Letter*, **68** (1), 199-222.

[27] Baker JW (2007): Quantitative classification of near-fault ground motions using wavelet analysis. *Bulletin of the Seismological Society of America*, **97** (5), 1486-1501.

[28] Bai YZ (2019): Comparison of the Recorded Significant Duration of the Lushan Earthquake with Empirical Model Predictions. *Bulletin of the Seismological Society of America*, **109** (6), 2325–2339.

